



Montréal, Québec

May 29 to June 1, 2013 / 29 mai au 1 juin 2013

Effects of Material Anisotropy and Geometric Imperfections on the Buckling Response of X100 UOE Pipes – A Finite Element Study

Muntaseer Kainat¹, Samer Adeeb¹, J. J. Roger Cheng¹, James Ferguson², Michael Martens²

¹Department of Civil and Environmental Engineering, University of Alberta

²TransCanada PipeLines Ltd.

Abstract: The use of high strength steel (HSS) pipes has increased in the past decades due to weight and cost reduction benefits. Cold forming processes, such as UOE, has become very popular due to its ease of pre-fabrication and mass production. The negative aspects associated with the cold forming of HSS pipes are the development of material anisotropy and geometric imperfections. The stress strain behavior of specimens obtained from the longitudinal and circumferential directions of an X100 line pipe differ significantly. It has been shown previously that the anisotropy of HSS can be related to the Bauschinger effect induced by the expansion process during cold forming. Analytical material models have been developed that can accurately predict the anisotropic behavior of HSS pipes. The geometric imperfections typically present in HSS UOE formed pipes have also been identified previously. The deviation of outer radii of pipes and the thickness variation of pipe wall can be defined with respect to the location of the longitudinal seam weld. This study combines the material anisotropy and geometric imperfections of HSS UOE formed pipes in a finite element model. The scope of the study includes determining the effects of material and geometric imperfections on the buckling response of HSS line pipes. Geometric imperfection models incorporating outer radii and wall thickness variation are developed and associated with the previously developed material model that imitates the anisotropic behavior. Wall thickness variation is seen to have a more profound effect on buckling response than radii variation. The buckling response is also seen to be sensitive to the direction of applied moment/rotation.

1 Introduction

The price of fossil fuel has increased with the increase in their demand in the last decade. As a result, the exploration of energy reserves in the sub-Arctic regions of North America has become an economically beneficial option. Consequently, the oil and gas industry is now an influential part of the Canadian economy. The industry accounts for exploration, extraction and transportation of oil and gas. Buried pipelines are considered to be a cheap and efficient form of transportation from the source to the point of consumption. Due to the harsh environmental conditions in the sub-Arctic regions, buried pipelines have

to pass through regions of discontinuous permafrost. The pipelines are subjected to differential settlements due to seasonal freeze-thaw cycles. The differential settlements impose bending stresses on pipe segments in addition to the stresses induced by internal and external pressure and differential temperature. These stresses are often responsible for the failure of pipeline.

In recent years, the use of high strength steel (HSS) pipes has increased due to its cost reduction benefits. Manufacturers are able to produce grades as high as X100, which has a Specified Minimum Yield Strength (SMYS) of 100 Ksi, or 690 MPa. The use of higher steel grades has resulted in the manufacturing of lighter pipe segments with higher diameter to thickness ratio as compared to normal grade steel pipes. The high strength large diameter pipes are generally manufactured by the UOE forming process. UOE is a cold forming process, where thin steel plates are first deformed into a U shape (U-forming), mechanically pressed in to an O shape (O-forming), and finally, expanded (E) into a cylindrical pipe segment. It has been found previously that the UOE forming process leaves the pipes with material, as well as geometric imperfections.

It has been revealed through experiments that the stress strain responses of HSS pipes are different for specimens obtained from the longitudinal and circumferential directions. The anisotropic behavior can either be the result of the inherent anisotropy of the plate material, or due to the deformations during the UOE manufacturing process. The geometric imperfections inflicted upon HSS pipes during UOE forming process have also been identified previously. It has been shown that HSS UOE formed pipes have distinct patterns of pipe wall thickness and outer radii variations. These patterns can be explained with respect to the location of the longitudinal seam weld in a pipe cross section, and it is possible to reproduce these patterns in the form of imperfection models.

2 Plastic Anisotropy in HSS UOE Pipes and Analytical Material Model

Adeeb et al. (2006) and Fatemi et al. (2008) have shown that HSS pipes show anisotropic plastic behavior, while normal strength pipes show isotropic behavior in both elastic and plastic range. The specimens taken from longitudinal direction show different stress strain response compared to those taken from the circumferential direction. The yield stress in the circumferential direction is higher than that in the longitudinal direction. The circumferential stress strain curve shows a distinct yield point, while the longitudinal stress strain curve has a more round shape and generally lies below the circumferential stress strain curve.

In UOE forming process, a steel plate is first bent into a U shape, and then a press is used to convert the U into an O shape. The plate is then welded in the longitudinal direction, and finally, it is expanded in the circumferential direction. The expansion process induces 2% circumferential plastic strain. The stress strain behavior of the tensile coupons taken from these pipes depends on the history of loading. When a UOE formed HSS pipe is loaded in the circumferential direction, its yield point will be higher than the original plate material. When loaded in the longitudinal direction, its yield point will be lower than that of the original plate material. This is a result of strain hardening and Bauschinger effect, typically exhibited by elastic-plastic material subjected to cyclic loading.

Neupane et al. (2012) were able to demonstrate that anisotropic behavior of HSS pipes can be modeled using a yield surface translation in the stress space. During the expansion stage in the manufacturing process, the yield centre moves in the stress space in the direction of increasing stress, i.e., the circumferential direction. Upon unloading and reloading, the yield point is expected to be higher than the original plate material in the circumferential direction, and lower in the longitudinal direction.

Neupane et al. (2012) were successful in developing a combined isotropic / nonlinear kinematic hardening model that can capture the plastic anisotropy of HSS pipes accurately. They approximated the virgin material curve from the available experimental stress strain data and calibrated the material parameters for the backstress evolution laws through an optimization scheme. Their developed material model can be incorporated into Finite Element Analysis (FEA) software such as ABAQUS.

3 Geometric Imperfections in X100 UOE Pipes

Measurement of geometric imperfections has been a major focus of study in energy pipelines. In previous years, researchers used physical measurement devices such as dial gauges and linear variable differential transducers (LVDT) to measure inner and outer radius of pipes from a reference axis. Bailey et al. (1984), Chen et al. (1993), DeCol et al. (1998), Dorey et al. (2001) are namely a few researchers who developed similar measurement devices using an assumed longitudinal axis and dial gauges or LVDTs to measure and map the actual surface imperfections of pipes.

Kainat et al. (2012) used a high resolution surface profiling device to create 3D profiles of large diameter HSS UOE pipes. They employed a 3D laser scanner to capture the inner and outer surfaces of pipes. They analyzed the acquired data in reverse engineering software to measure the different geometric attributes of the pipes. They were able to identify typical patterns of imperfection in X100 UOE pipes.

Kainat et al. (2012) were able to identify different patterns for pipe wall thickness variation and outer radii variation in HSS UOE pipes. They observed that pipe wall thicknesses are less than the specified value near the seam weld; increases beyond the specified value away from the seam weld, and approaches the maximum value about halfway around the perimeter. They also compared the actual pipe geometry with an ideal pipe of constant radius to observe the radii variation patterns. They were able to detect wavy patterns of radii variation which can be described with respect to the location of the seam weld. The imperfections reported by Kainat et al. (2012) can be expressed numerically and used in FEA models.

4 FEA Model

This study focuses on investigating the effects of the two key features of HSS UOE pipes through FEA models: material anisotropy, and imperfect geometry. The study is limited to X100 Pipes with 1067 mm specified outer diameter (OD) and 14.275 mm specified pipe wall thickness. The material model and geometric imperfections used in this study are discussed in the subsequent sections.

4.1 Anisotropic Material Model

The material model developed for X100 pipes by Neupane et al. (2012) is used in this study. The tension coupons were obtained from an X100 pipe of 762 mm OD and 12.7 mm wall thickness. An analytical virgin material curve is first developed from the circumferential stress strain data obtained from tension test. Armstrong-Frederick law (Armstrong et. al., 1966) is chosen for backstress evolution, and the material parameters corresponding to the specific pipe, as optimized and presented by Neupane et al. (2012) are used to calculate the values of backstress at different plastic strain values. The assumed virgin material curve, the parameters, and the backstress values along with the Elastic Modulus and Poisson's ratio altogether define the anisotropic material model.

The material model is input into ABAQUS to verify the expected anisotropic behavior. Two methods are applied for this purpose. First, the material model is assigned to a single four node, rectangular, plane stress shell element. To simulate the expansion process during manufacturing, an initial condition is introduced to the model. 2% plastic strain and the corresponding backstress value from Armstrong-Frederick law are assigned as initial conditions in the circumferential direction. The element is then loaded in longitudinal and circumferential directions separately to observe its stress strain response.

Next, the material model is assigned to a 3D cylindrical shell representing a pipe of 1067 mm OD, along with the initial conditions simulating the expansion process. The cylinder is then loaded in the longitudinal and circumferential directions by applying axial tension and internal pressure separately. The stress strain responses of an element on the pipe are then observed. The stress strain curves from tensile tests and FEA results are shown in Figure 1.

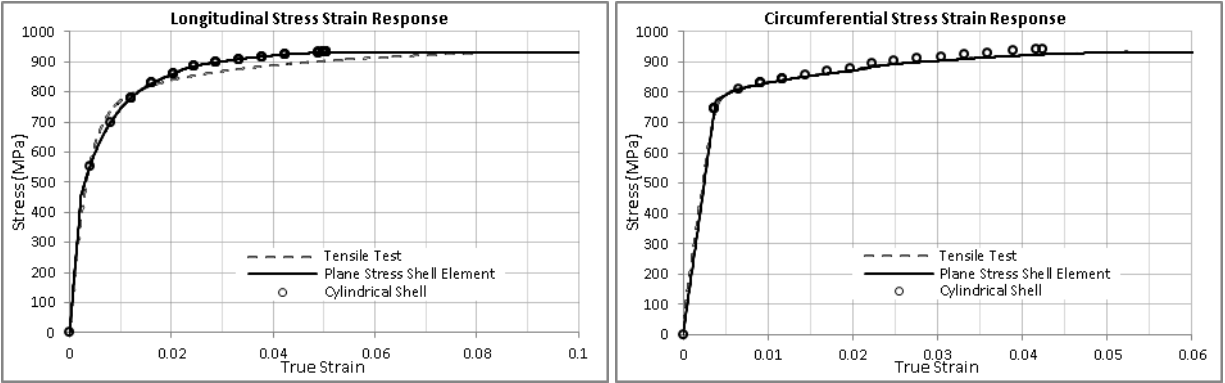


Figure 1: Comparison of actual stress strain response in longitudinal and circumferential directions with the FEA results of anisotropic material model

Figure 1 confirms the close resemblance of stress strain response between the anisotropic material model and the actual test data in both longitudinal and circumferential directions.

4.2 Geometric Imperfection Models

The geometric imperfections corresponding to pipe wall thickness variation and outer radii variation, as found by Kainat et al. (2012) are employed in the imperfection models. The development of the model is elaborated in the following sections.

4.2.1 Pipe Wall Thickness Variation

Pipe wall thickness variations are expressed in terms of angles around the centre of the pipe cross section. A line connecting the centre and the point on the pipe cross section corresponding to the location of the longitudinal seam weld is considered to be the reference line. The angles are measured in counter clockwise direction with respect to the reference line. Wall thickness values are assigned to each angle. The thickness variations are then expressed as percentages of the specified wall thickness. A regression analysis is performed to fit a curve to the measured thickness variation. The equation obtained from the regression analysis is then manipulated to find a better fit to the measured values. The equation is as follows:

$$\% \text{ Thickness Variation} = 3 - 16 \cos (1.2 \theta) + 12 \sin (0.7 \theta) \quad [1]$$

where the angle θ is in radians. The actual measured thickness variations and the fitted curve from Equation 1 are shown in Figure 2.

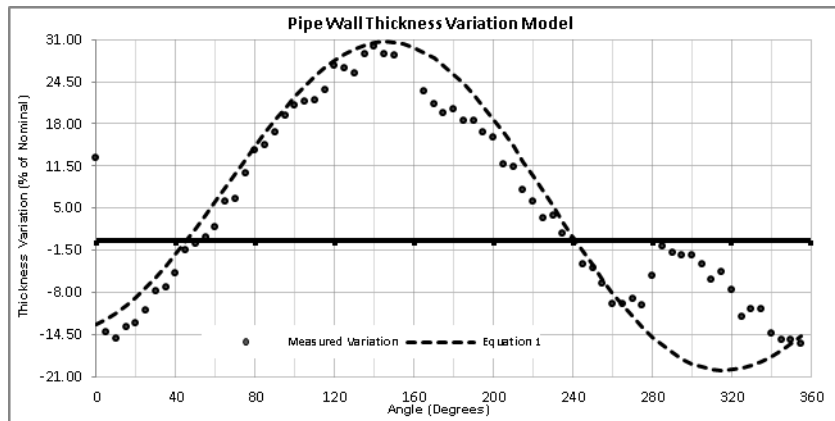


Figure 2: Measured pipe wall thickness variation and fitted curve from Equation 1

The pipe is modeled in ABAQUS as a cylindrical shell of constant radius. The shell thickness is defined in a cylindrical coordinate system, such that,

$$\text{Thickness} = \text{Specified Thickness} \times (1 + \% \text{ Thickness Variation from Equation 1}) \quad [2]$$

4.2.2 Outer Radii Variation

Kainat et al. (2012) reported the radii variation as the percentage of specified radius and in terms of angles about the reference line mentioned in the previous section. To express the variation mathematically, again a regression analysis is performed, and the obtained equation is adjusted to find a good fit between the measured and numerical values. The equation is as follows:

$$\% \text{ Outer Radii Variation} = -0.46 - 0.13 \cos(0.6 \theta) + 1.35 \sin(\theta) \quad [3]$$

The actual measured radii variations and the fitted curve from Equation 3 are shown in Figure 3.

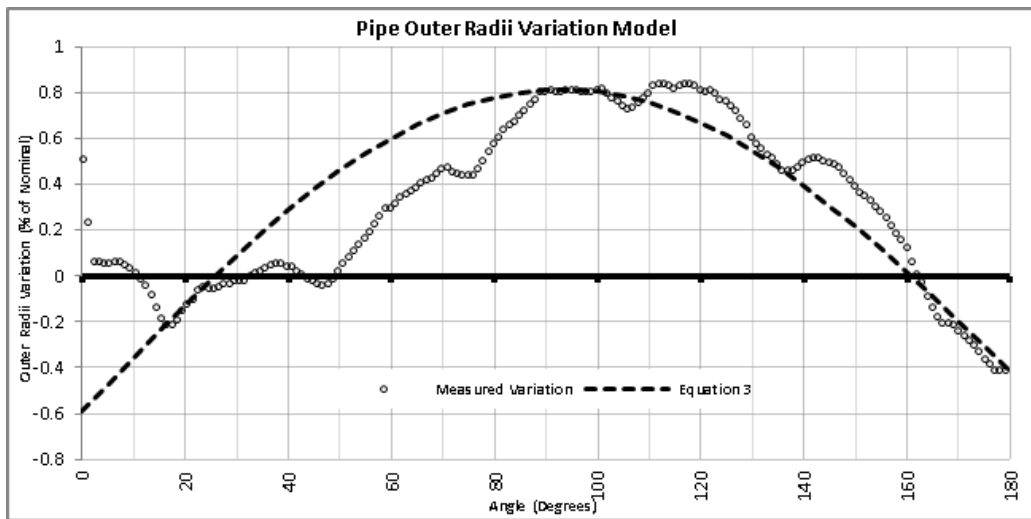


Figure 3: Measured Outer radii variation and fitted curve from Equation 2

Again, a cylindrical shell is modeled in ABAQUS with variable outer radii values. The variations are calculated from Equation 3.

5 Finite Element Analysis Results

Different pipe models are developed to observe the effects of material anisotropy and geometric imperfections individually and as combinations. The length of the pipe is taken as 5 OD. S4R shell elements are used for the pipe model. Mesh size is selected as 40 mm by 40 mm. The pipe is fixed at one end, and a concentrated rotation is applied at the other end. Pipes are analyzed for unpressurized and pressurized conditions. For pressurized condition, a uniform internal pressure is applied that corresponds to a Hoop stress of 80% of SMYS. Riks method is applied to solve the non-linear buckling analysis due to applied rotation at one end. From the moment-rotation curve for each case, the peak moment and the corresponding end rotation are observed, which signify the onset of buckling due to pure bending.

The shell thickness deviation assigned to the FEA model, along with its boundary conditions are shown in Figure 4. The typical buckling shapes for pipes with and without internal pressure are shown in Figure 5. Unpressurized pipes buckle in diamond shape, where the pipe wall buckles inward at mid length. Pressurized pipes buckle in bulge shape, where the pipe wall protrudes outward near the end where rotation is applied.

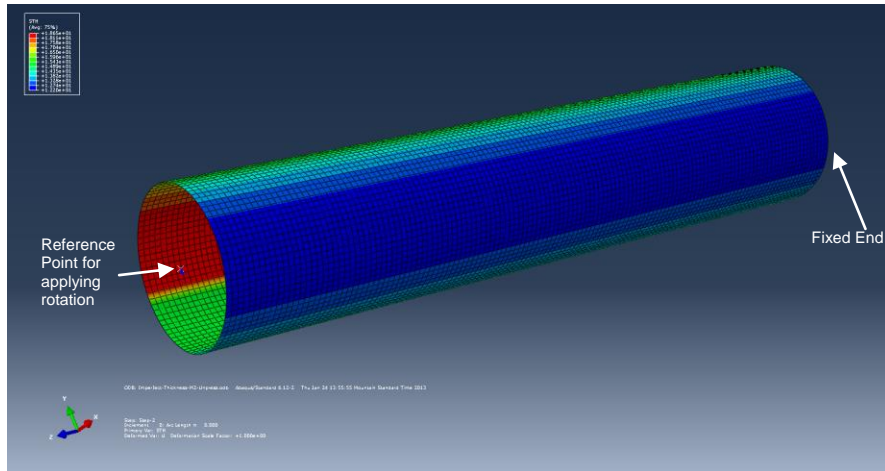


Figure 4: Shell thickness spectrum and boundary conditions applied to the FEA model

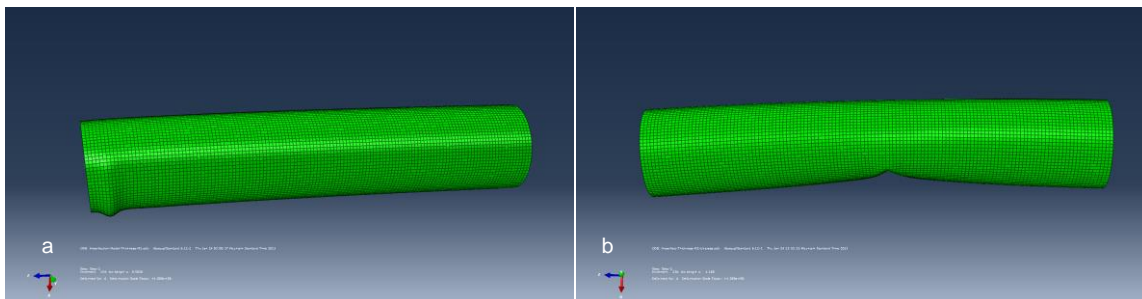


Figure 5: Typical buckling mode for a) Pressurized pipe, and b) Unpressurized pipe

5.1 Effect of Material Anisotropy

Three material models are studied for comparison. One anisotropic model, as discussed previously, one isotropic model that corresponds to the stress strain behavior in the longitudinal direction of the pipe, and another isotropic model that corresponds to the stress strain behavior in the circumferential direction of the pipe. The material models are assigned to a pipe of uniform OD and wall thickness. Therefore, the different responses obtained from these pipes are solely due to the effect of different material models. The moment-rotation responses for different materials are shown in Figure 6.

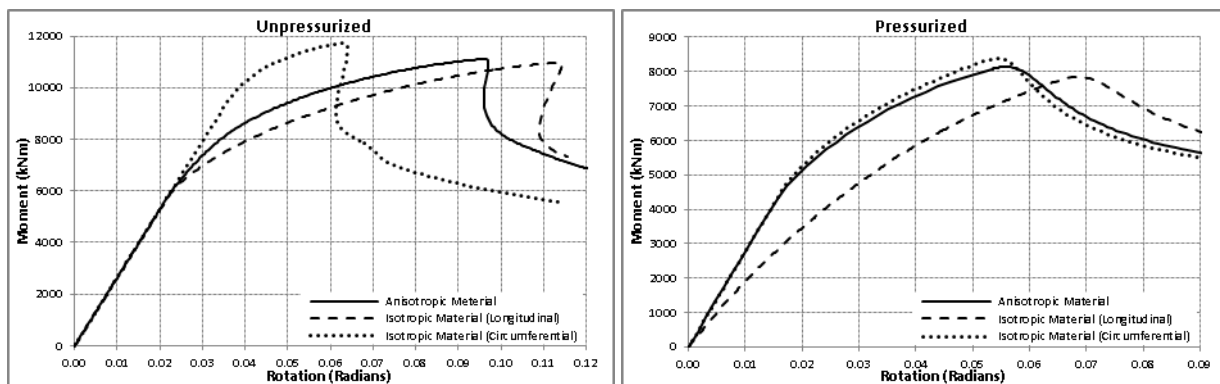


Figure 6: Moment-Rotation responses of isotropic and anisotropic material models

From Figure 6, it is seen that for unpressurized condition, peak moment and end rotations corresponding to the longitudinal isotropic model are respectively 1.28% lower and 17.92% higher than that corresponding to the anisotropic model. The circumferential isotropic model, however, shows 5.64% higher peak moment and 34.61% lower end rotation when compared to the anisotropic model.

For pressurized condition, the longitudinal isotropic model produces 3.8% lower peak moment and 24.7% higher end rotation, and the circumferential isotropic model produces 2.85% higher peak moment and 3.89% lower end rotation compared to those of the anisotropic model.

5.2 Effect of Pipe Wall Thickness Variation

The pipe wall thickness variation model is combined with the anisotropic material model. The moment-rotation response is expected to be sensitive to the direction of the applied rotation. The direction from the centre of the pipe cross section to the location of the seam weld is considered as direction 1. Direction 3 is the longitudinal direction of the pipe. The schematics of different directions of applied rotation, and the moment-rotation responses for different directions are shown in Figure 7.

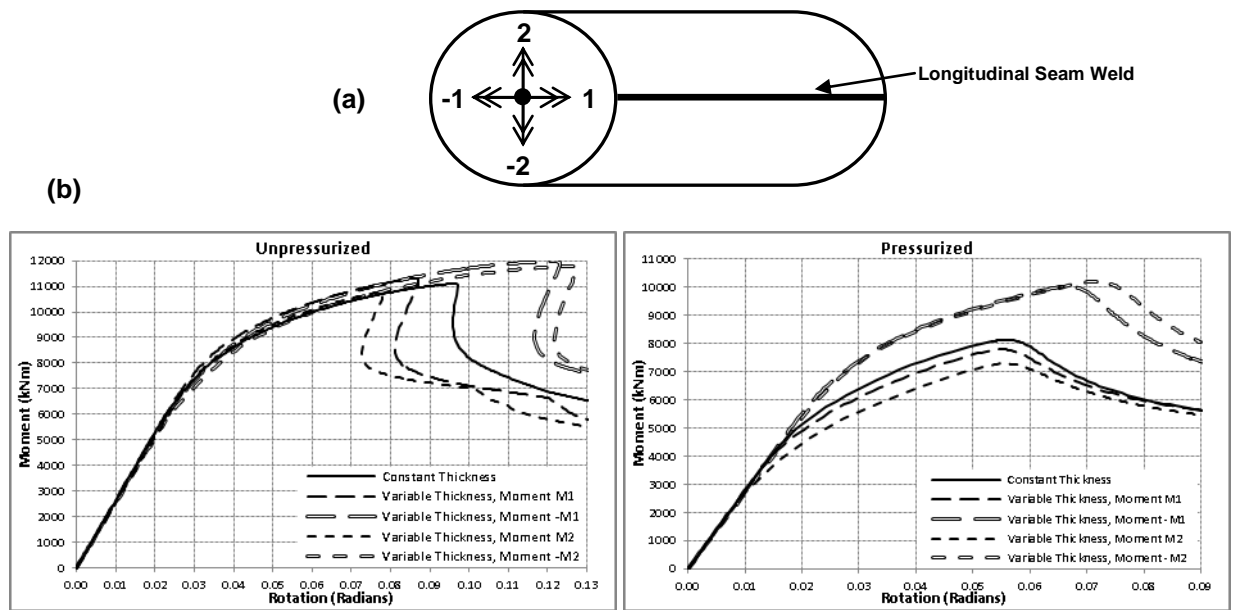


Figure 7: (a) Schematics of the directions of applied rotation, (b) Moment-Rotation responses in different directions for pipe wall thickness variation

The differences in peak moment and end rotation values corresponding to each direction compared to the responses corresponding to constant thickness model are listed in Table 1:

Table 1: Differences in peak moment and end rotations corresponding to different directions as percentages of ideal response (constant thickness model)

		Unpressurized		Pressurized	
		% Difference		% Difference	
		Peak Moment	End Rotation	Peak Moment	End Rotation
Direction	1	1.91%	-9.93%	-4.21%	-1.68%
	-1	7.79%	26.18%	23.35%	19.14%
	2	-2.90%	-19.73%	-10.49%	-0.17%
	-2	5.96%	30.21%	25.42%	27.83%

It is observed that there is a reduction of peak moment and end rotation values for both unpressurized and pressurized conditions when the applied rotation is in direction 2. Therefore, direction 2 is deemed the weakest direction of rotation or moment application compared to the other three directions.

5.3 Effect of Radii Variation

The radii variation model is combined with the anisotropic material model. The moment rotation responses in directions 1 and 2 as compared to the constant radius model are shown in Figure 8:

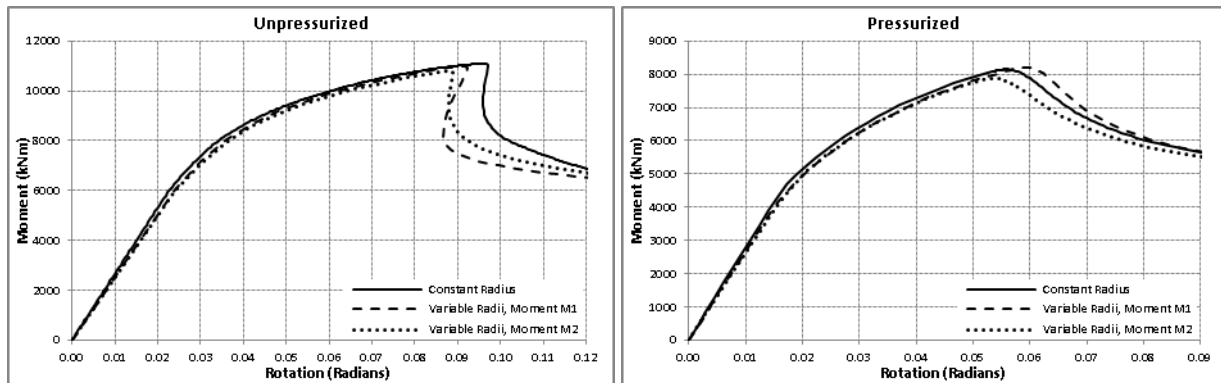


Figure 8: Moment-Rotation responses for radii variation

Similar to the thickness variation model, the radii variation exhibits weakest response in direction 2. For unpressurized condition, the peak moment and end rotation values are reduced by 2.84% and 8.26% respectively from the constant radius model. For pressurized condition, the reductions are 3.34% in peak moment and 4.47% in end rotation.

6 Discussion

From the moment rotation responses pertaining to different material and geometric models, it is observed that, the mode of buckling is different for pressurized and unpressurized pipes. Unpressurized pipes have higher peak moment and end rotation values for all cases compared to pressurized pipes. Unpressurized pipes buckle inward at mid length, while pressurized pipes buckle with outward protuberance at the end where rotation is applied. These modes are termed diamond mode and bulge mode respectively, and are typical to unpressurized and pressurized pipe buckling.

The moment rotation response corresponding to the anisotropic material model tends to lie in between those of the two isotropic material models using longitudinal and circumferential stress strain data. For unpressurized condition, the isotropic material model with longitudinal stress strain data is closer to the anisotropic model with -1.28% and +17.92% differences in peak moment and end rotation values. For pressurized condition, the isotropic material model with circumferential stress strain data is closer to the anisotropic model with +2.85% and -3.89% differences in peak moment and end rotation values.

The pipe wall thickness variation models suggest that the behavior of the pipe is sensitive to the direction of the applied rotation/moment. Direction 2 shows the weakest response in both pressurized and unpressurized conditions, where compressive stresses develop in the regions of the pipe wall with reduced thickness values. In direction 2, the end rotation is reduced by 19.73% in unpressurized condition and the peak moment is reduced by 10.49% in pressurized condition. For both conditions, the rest three directions either show higher peak moment, or the reduction is within 5% of constant thickness model. Regarding end rotations, the rest three directions either show higher end rotations, or the reduction is within 5% of constant thickness model, except for direction 1, where the end moment is reduced by 9.93%. Considering the wide range of end rotation difference values, a reduction of less than 10% is assumed acceptable.

The radii variation models showed that the peak moment and end rotation values corresponding to direction 2 are less than those corresponding to direction 1. This is due to the fact that, in direction 2, the imperfect OD is less than the specified OD, and in direction 1, it is greater than the specified OD. For both pressurized and unpressurized conditions, the reductions in peak moments and end rotations are within 5% and 10% respectively when applied rotation is in direction 2.

The different buckling modes corresponding to pressurized and unpressurized pipes observed in this study are similar to previous FEA studies carried out by other researchers. The effects of material anisotropy and its difference in response from the isotropic material models also agree with the findings of Neupane et al. (2012). Kainat et al. (2012) reported their measured radii variations to be within the CSA Z662 specified tolerance, and from the FEA studies, it is seen that, the radii variations truly have negligible effects on the moment rotation responses. The thickness variation patterns, however, have pronounced impact on the buckling response. It is observed that, the buckling response is sensitive to the direction of rotation or applied moment. Pipes are weakest in direction 2, where compression develops in the regions of the pipe wall with reduced wall thickness and outer radius. These regions are near the vicinity of the longitudinal seam weld of the pipe.

7 Conclusions and Future Work

This study successfully showed the effects of material anisotropy and geometric imperfections on the buckling response of X100 UOE pipes. From the analysis results, it is concluded that, pipe wall thickness variations are a bigger issue compared to radii variations in X100 UOE pipes. The pipe wall thickness variations typically present in X100 UOE pipes tend to make them weaker when moment or rotation is applied in a particular direction. This direction corresponds to compression in the pipe cross section near the vicinity of the longitudinal seam weld.

This study was limited to 1067 mm specified OD and 14.275 mm thick walled pipe. Further analysis on different pipe sizes can be carried out to capture the full picture regarding the effects of imperfection. This study was limited to modeling measured initial imperfections of pipes prior to being in service. The development of ovalization due to pipe bends and their corresponding effects were beyond the scope of this study. This study ignored the effects of the geometry and the material properties of the longitudinal seam weld. Further study may prove whether considering the seam weld in the FEA model will have any effects on the buckling response.

8 References

- Bailey, R. and Kulak, G.L. 1984. Flexural and Shear Behaviour of Large Diameter Steel Tubes. *Structural Engineering Report No. 119*, Department of Civil Engineering, University of Alberta, Edmonton, Alberta, Canada.
- Chen, Q., Elwi, A.E. and Kulak, G.L. 1993. Bending Strength of Longitudinally Stiffened Steel Cylinder. *Structural Engineering Report No. 192*, Department of Civil Engineering, University of Alberta, Edmonton, Alberta, Canada.
- DeCol, P.R., Grondin, G.Y., Cheng, J.J.R. and Murray, D.W. 1998. Behaviour of Large Diameter Line Pipe Under Combined Loads. *Structural Engineering Report No. 224*, Department of Civil Engineering, University of Alberta, Edmonton, Alberta, Canada.
- Dorey, A.B., Cheng, J.J.R. and Murray, D.W. 2001. Critical Buckling Strains in Energy Pipelines. *Structural Engineering Report No. 237*, Department of Civil Engineering, University of Alberta, Edmonton, Alberta, Canada.
- Sen, M. 2006. Behaviour of Cold Bend Pipes under Combined Loads. *PhD. Dissertation*, Department of Civil and Environmental Engineering, University of Alberta, Edmonton, Alberta, Canada.
- Zhang, J. 2010. Development of LCF Life Prediction Model for Wrinkled Steel Pipes. *PhD. Dissertation*, Department of Civil and Environmental Engineering, University of Alberta, Edmonton, Alberta, Canada.
- Armstrong, P.J., Frederick, C. O., 1966. A Mathematical Representation of Multiaxial Bauschinger Effect. Report RD/B/N731, CEGB, Central Electricity Generating Board, Berkeley, UK.
- Bauschinger, J., 1886, Elastic limit, American Engineering.

- Broggiato, G.B., Campana, F., Cortese, L., 2008. The Chaboche Nonlinear Kinematic Hardening Model: Calibration Methodology and Validation. *Meccanica* 43, 115-124.
- Canadian Standards Association, 2007. Z662-07 Oil and Gas Pipeline Systems. Canadian Standards Association, Etobicoke, Ontario
- Chaboche, J.L., 1989. Constitutive Equations for Cyclic Plasticity and Viscoplasticity. *Int. J. Plasticity* 5, 247-302.
- Hill, R., 1948. A Theory of the Yielding and Plastic Flow Of Anisotropic Metals. *Proc. R. Soc. Lond. A* 193, 281-297.
- Adeeb, S., Zhou, J., Horsley, D., 2006, Investigating the effect of UOE forming processes on the buckling of line pipes using finite element modeling. *Proc. of IPC 2006*, Calgary, Alberta, Canada, Sept 25-29
- Fatemi, A., Kenny, S., Sen, M., Zhou, J., Taheri, F., Paulin, M., 2008, Investigations on the Local Buckling Response of High Strength Linepipe, *Proc. of IPC 2008*, Calgary, Alberta, Canada, Sept 29-Oct 3, 2008.
- Neupane, S., Adeeb, S., Cheng, R., Ferguson, J., Martens, M., 2012. Modeling the Deformation Response of High Strength Steel Pipelines. *Transaction of the ASME, Journal of Applied Mechanics*, September 2012.
- Kainat, M., Adeeb, S., Cheng, R., Ferguson, J., Martens, M., 2012. Measurement of Initial Imperfection of Energy Pipeline Using 3D Laser Scanner. *Proc. of CSCE 2012*, Edmonton, Alberta, Canada.
- Kainat, M., Adeeb, S., Cheng, R., Ferguson, J., Martens, M., 2012. Identifying Initial Imperfection Patterns of Energy Pipes Using A 3D Laser Scanner. *Proc. of IPC 2012*, Calgary, Alberta, Canada.